



http://pubs2.ascee.org/index.php/ijrcs



A Combination of HHO and BEI Techniques for Frequency Control in Renewable-Dominated Microgrids: Towards Advancing Sustainable Development

Mohamed F. Elnaggar a,1,*

- ^a Department of Electrical Engineering, College of Engineering, Prince Sattam Bin Abdulaziz University, Al-Kharj 11942, Saudi Arabia
- 1 mfelnaggar@yahoo.com
- * Corresponding Author

ARTICLE INFO

Article history

Received May 24, 2025 Revised August 05, 2025 Accepted October 14, 2025

Keywords

Sustainable Development; Microgrids; Load Frequency Control; Renewable Energy Sources; Harris Hawks Optimization with the Balloon Effect

ABSTRACT

To address the rising need for resilient and eco-friendly power systems, this research presents an intelligent load frequency control (LFC) framework specifically designed for hybrid microgrids with significant renewable energy integration and variable operational dynamics. The proposed control scheme leverages the Harris Hawks Optimization (HHO) algorithm in conjunction with a Balloon Effect (BE) adaptation mechanism, enabling real-time tuning of controller parameters in response to system fluctuations and disturbances. The simulation model encompasses a diverse hybrid microgrid configuration, comprising PV arrays, a diesel generator, and time-varying load profiles. Performance assessments were conducted across three operating modes: diesel-alone supply, coordinated diesel-PV operation, and a high-renewable scenario incorporating uncertainties in system inertia, damping, and droop. In all tested cases, the HHO + BE controller demonstrated superior behavior compared to standard optimization techniques like GTO, SCA, and WOA, exhibiting quicker stabilization, smaller frequency deviations (down to ± 0.18 Hz), and minimized control actions. Overall, this study underscores the adaptability and reliability of the HHO + BE control approach for maintaining frequency stability in modern, low-inertia microgrids. The results offer compelling evidence of its effectiveness in real-time applications, particularly in environments increasingly dominated by fluctuating renewable energy sources and uncertain operating conditions.

This is an open-access article under the CC-BY-SA license.



1. Introduction

Amid increasing environmental concerns and the urgent need to combat climate change, there has been a growing global movement toward cleaner energy alternatives [1]-[3]. Conventional fossilfueled power plants, while historically dominant, contribute significantly to ecological degradation through carbon emissions and excessive water consumption [4]-[7]. In contrast, renewable energy technologies (such as PV, concentrated solar power (CSP), wind turbines, and hydrogen systems) are now integral to global energy transformation efforts [8], [9]. These technologies are not only environmentally friendly but also becoming more economically viable [10], [11]. For example, the global deployment of PV systems in 2021 alone prevented nearly 270 million metric tons of CO2





from entering the atmosphere [12]. Additionally, the use of PV mitigates air pollution and conserves water by eliminating the need for cooling processes typical of thermal plants [13], [14]. However, the variability and unpredictability of renewable energy output pose substantial challenges to system operators, especially in stand-alone or weakly interconnected power systems [15], [16]. To address this, MGs have been introduced as a decentralized solution for integrating distributed energy resources (DERs) [17]. These small-scale, flexible systems can function independently (islanded mode) or alongside the main grid. Nevertheless, maintaining voltage and frequency stability within islanded MGs remains a major technical hurdle due to reduced inertia and the prevalence of power-electronic interfacing [18].

In power systems characterized by low inertia, such as islanded MGs, abrupt shifts in load demand or renewable generation can trigger sharp frequency variations. These fluctuations threaten operational stability and system security [19]-[21]. Relying on fixed-parameter controllers such as conventional PI regulators is often insufficient in such volatile environments, especially where nonlinear dynamics and uncertainties are prevalent [22], [23]. This underscores the need for advanced, intelligent control systems that can adapt in real time [24]. Among various optimization techniques, bio-inspired algorithms have demonstrated impressive capabilities in enhancing system performance under uncertain and nonlinear conditions [25], [26]. Specifically, the HHO algorithm has gained recognition for its efficient balance between exploration and exploitation in complex optimization tasks [27], [28]. HHO is inspired by the cooperative hunting behavior of Harris's hawks and has shown superior convergence characteristics when applied to energy and control applications [25], [29], [30]. Recent studies have successfully integrated bio-inspired algorithms into smart grid control schemes and frequency regulation strategies, particularly under high-RES penetration and islanded operation conditions [31]-[33]. This research is motivated by the potential of HHO to provide a flexible, responsive solution for frequency control in hybrid MGs subject to real-world uncertainties.

While numerous optimization algorithms have been proposed for LFC in MGs (including GTO [34], SCA [35], and WOA [36]), many fall short when subjected to highly dynamic or uncertain operating conditions. These techniques often suffer from slow convergence or limited robustness, especially under nonlinearities and cyber disturbances [25], [37]. Moreover, their performance under HIL conditions or real-time operational disturbances is not well characterized, which limits their practical deployment in smart MGs [38]-[41]. Although the HHO algorithm has proven successful in diverse engineering fields (thanks to its powerful balance between exploration and exploitation [42]), its application in real-time adaptive frequency control of hybrid MGs is still underexplored [43], [44], [15]. More critically, there is a notable lack of comprehensive comparative studies that evaluate HHO's resilience against alternatives like GTO, SCA, and WOA in both simulated and experimental settings [45]-[47]. Most existing work is limited to simulation-based studies without hardware verification, creating a gap in experimental validation and real-world applicability [48], [49]. Moreover, modern grid dynamics demand adaptive controllers capable of withstanding renewable intermittency, nonlinear behaviors, and external disturbance conditions under which bioinspired techniques like HHO are theoretically suited but practically underutilized [50]-[53]. To highlight these considerations, Table 1 provides a comparative overview of the key performance metrics such as convergence speed, tracking accuracy, and adaptability (across HHO, GTO, SCA, and WOA). This study proposes an enhanced LFC strategy for hybrid microgrids based on the HHO algorithm, augmented with a BE mechanism. The proposed method adaptively tunes controller parameters in real time to counteract fluctuations in both load demand and renewable energy generation. A hybrid MG model consisting of PV arrays, DGs, and varying load conditions serves as the testing environment. The specific contributions of this research are outlined as follows:

- Formulation of an adaptive LFC framework using HHO for robust frequency regulation under dynamic and uncertain operating conditions;
- Integration of a BE mechanism into HHO to improve the algorithm's sensitivity to disturbances and parameter changes, enhancing its responsiveness and adaptability;

- Comparative performance evaluation of the proposed HHO+BE approach against three wellestablished metaheuristic algorithms (GTO, SCA, and WOA) based on accuracy, convergence, and control stability;
- Demonstration of superior dynamic response and improved robustness of the HHO+BE controller in handling nonlinearities and maintaining frequency stability in low-inertia MG environments.

Algorithm	Exploration– Exploitation Balance	Convergence Speed	Adaptability to Uncertainty	Suitability for Real-Time Control	Prior Application in LFC
HHO [54]	Excellent (dynamic switching strategy)	High	Strong (adaptive behavior in nonlinear settings)	Suitable (lightweight and responsive)	Limited (emerging research area)
GTO [55]	Good (based on social hierarchy)	Moderate	Moderate (requires parameter tuning)	Moderate (computational overhead exists)	Moderate (recent applications in hybrid systems)
SCA [56]	Moderate (periodic pattern)	Fast in early stages, weak in exploitation	Weak (sensitive to noise)	Less Suitable (may require hybridization)	High (widely studied in literature)
WOA [57]	Good (encircling and bubble-net mechanism)	Moderate to slow	Moderate (may suffer premature convergence)	Limited (slow response under real-time loads)	High (used in several LFC scenarios)

Table 1. Comparative analysis of metaheuristic algorithms for LFC in MGs

2. Dynamic Modeling Framework and Optimization Strategies

2.1. Power System Modeling

Fig. 1 illustrates the block representation of the MG power system under study. The system's dynamic behavior is characterized by a set of mathematical equations, as outlined in [58], [59]. Specifically, the interaction between power generation and load demand is modeled through the relationship between the net power imbalance ($\Delta Pd - \Delta PL$) and the resulting frequency deviation (Δf), which captures the system's dynamic response to mismatches in supply and demand [58], [59].

$$f = \left(\frac{1}{M}\right) \cdot \Delta P d - \left(\frac{1}{M}\right) \cdot -\Delta P L - \left(\frac{D}{M}\right) \cdot \Delta f \tag{1}$$

The dynamic behavior of the DG is formulated as follows:

$$\Delta Pd = \left(\frac{1}{Td}\right) \cdot \Delta Pg - \left(\frac{1}{Td}\right) \cdot \Delta Pd \tag{2}$$

The governing system dynamics are represented by the following expression:

$$\Delta Pg = \left(\frac{1}{Tg}\right) \cdot \Delta Pc - \left(\frac{1}{R \cdot Td}\right) \cdot \Delta f - \left(\frac{1}{Tg}\right) \cdot \Delta Pg \tag{3}$$

The dynamic performance of the MG system is shaped by a set of interrelated variables and parameters. In this framework, ΔPg refers to the alteration in the governor output, ΔPd signifies the change in diesel generator power, and Δf indicates the deviation in system frequency. These variations are primarily influenced by load fluctuations (ΔPL) and corrective actions introduced through the supplementary control input (ΔPc). The dynamic response of the system is further determined by intrinsic physical constants, notably the equivalent inertia (M), which affects resistance to frequency shifts, and the damping factor (D), which modulates oscillation decay. Additionally, the governor's responsiveness to frequency deviation is modeled by the droop coefficient (R), while the dynamic delays associated with the governor and turbine are captured by

their respective time constants, Tg and Td. To describe how these quantities evolve, the model incorporates differential expressions (namely $(\frac{df}{dt}, \frac{dPd}{dt}, \frac{dPg}{dt})$) representing the rate of change of frequency, DG power, and governor action, respectively.

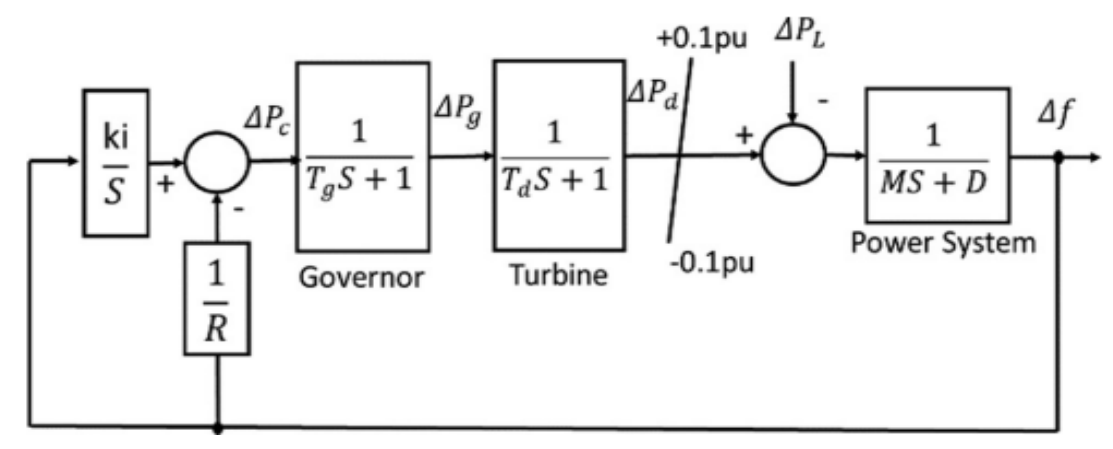


Fig. 1. Dynamic model architecture of the MG power system [60]

2.2. HHO Method

The HHO is a bio-inspired, population-based heuristic designed to mimic the cooperative hunting strategies of HH in nature. Originally developed in [61], [62], this algorithm draws on the agile, tactical movements hawks use to corner prey, incorporating both individual pursuit and collective coordination. One of HHO's most distinguishing features is its adaptive control over exploration and exploitation processes, which depend on a dynamic variable representing the prey's escaping energy. A schematic overview of this behavior is depicted in Fig. 2, capturing the algorithm's operational workflow. The optimization cycle begins by randomly positioning hawks across the solution landscape. The transition between global search (exploration) and local refinement (exploitation) is governed by the escaping energy E, calculated as:

$$E = 2E_0 \left(1 - \frac{t}{T} \right) \tag{4}$$

where E_0 is a random number in the range [-1, 1], t is the current iteration, and T is the maximum number of iterations. When the absolute value of E satisfies $|E| \ge 1$, the algorithm prioritizes exploration, encouraging hawks to probe diverse areas of the search space. During this phase, position updates are performed using strategies such as:

$$\mathbf{x}_{t+1} = \begin{cases} \mathbf{X}_{\text{rend}} - r_1 \cdot \mathbf{X}_{\text{anad}} - 2r_2 \cdot \mathbf{X}_t \mid , \text{ if } r \ge 0.5 \\ \\ (\mathbf{X}_{\text{bet}} - \mathbf{x}) - r_3 \cdot (LB + r_4(UB - LB)), \text{ if } r < 0.5 \end{cases}$$
 (5)

As the value of |E| falls below 1, the algorithm shifts into exploitation mode, choosing one of several strategies based on random probabilities and the prey's remaining energy. These strategies include:

Soft besiege:

$$X_{t+1} = \Delta X_t - E \mid JX_{\text{hest}} - X_t \mid \tag{6}$$

Hard besiege:

$$X_{t+1} = X_{\text{best}} - E \cdot |\Delta X_t$$
 (7)

Soft besiege with progressive, rapid dives:

$$Y = X_{\text{best}} - E \cdot |J \cdot X_{\text{best}} - X_t|$$
 (8)

Hard besiege with progressive rapid dives:

$$Z = Y + S \cdot Levy(d) \tag{9}$$

This iterative process continues until the maximum number of iterations is reached, at which point the algorithm returns the best solution as the global optimum. The HHO algorithm's ability to balance extensive search with deep exploitation (especially through mechanisms like Lévy flights) makes it a powerful tool for tackling complex, nonlinear optimization problems often encountered in energy systems and control engineering.

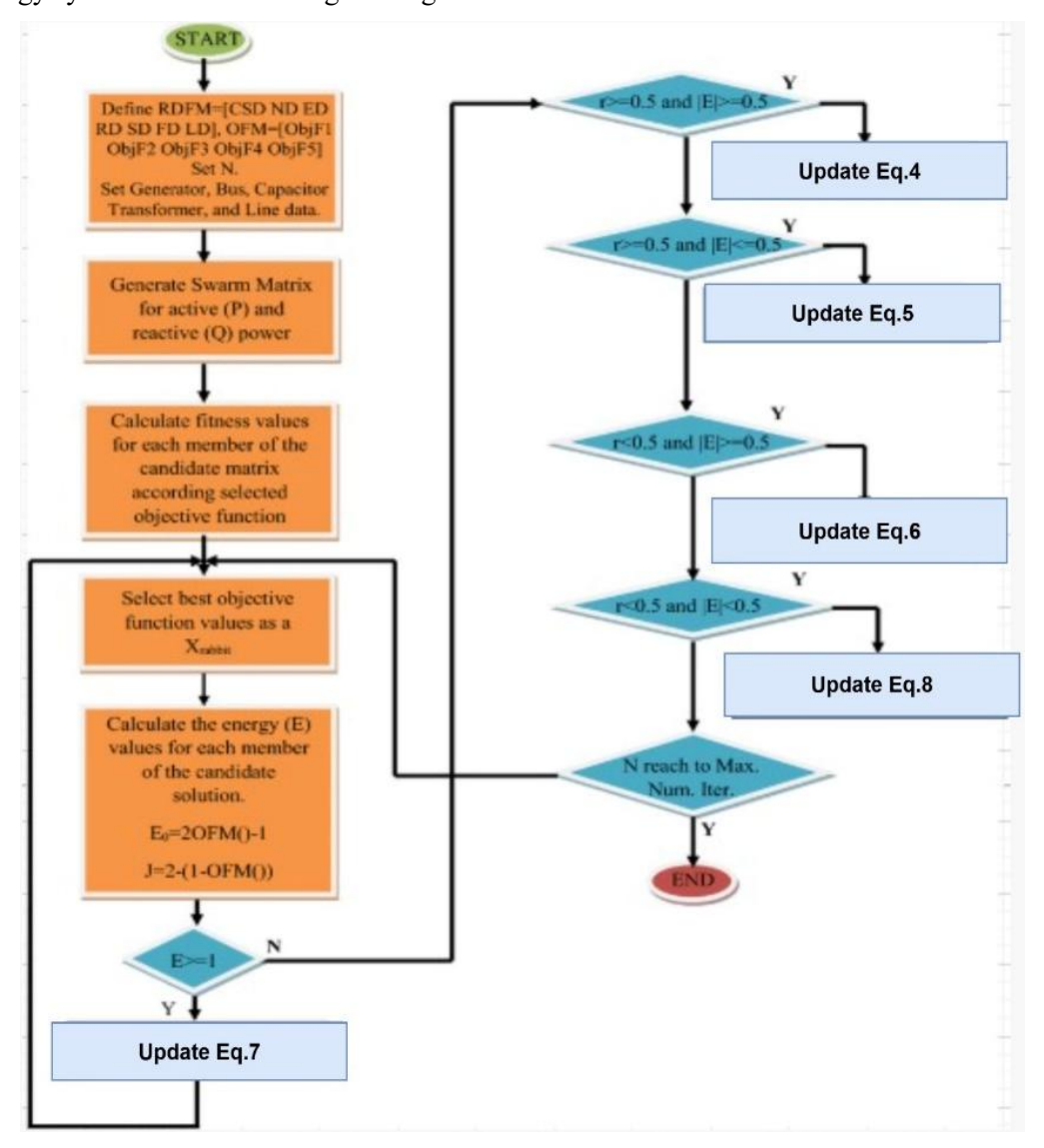


Fig. 2. HHO flowchart [63]

2.3. BEI Technique

The BE concept originates from the behavior of air pressure on a balloon's volume, where slight changes in pressure cause significant expansion or contraction. Analogously, in control systems, external disturbances and parameter uncertainties can substantially influence the dynamic behavior of the system's transfer function, denoted as. As depicted in Fig. 3, the integration of the BE mechanism plays a pivotal role in refining the optimization algorithm's objective function throughout iterative processes, thereby boosting its overall effectiveness [64], [65]. At each iteration, the

microgrid's system behavior can be described by an online transfer function, defined as the ratio between the output and the input:

$$G_i(s) = \frac{Y_i(s)}{U_i(s)} \tag{10}$$

Moreover, the transfer function at iteration evolves from its previous state, scaled by a variable gain factor:

$$G_i(s) = AL_i G_{i-1}(s) \tag{11}$$

Here, it is itself linked to the nominal system transfer function through another adaptive scaling parameter:

$$G_{i-1}(s) = \rho_i G_0(s) \tag{12}$$

This recursive structure allows the algorithm to adapt dynamically by modifying the system model in response to evolving operational conditions, enabling more accurate and responsive control over time.

Where

$$\rho_i = \prod_{n=1}^{i-1} AL_n \tag{13}$$

$$G_i(s) = AL_i \rho_i G_0(s) \tag{14}$$

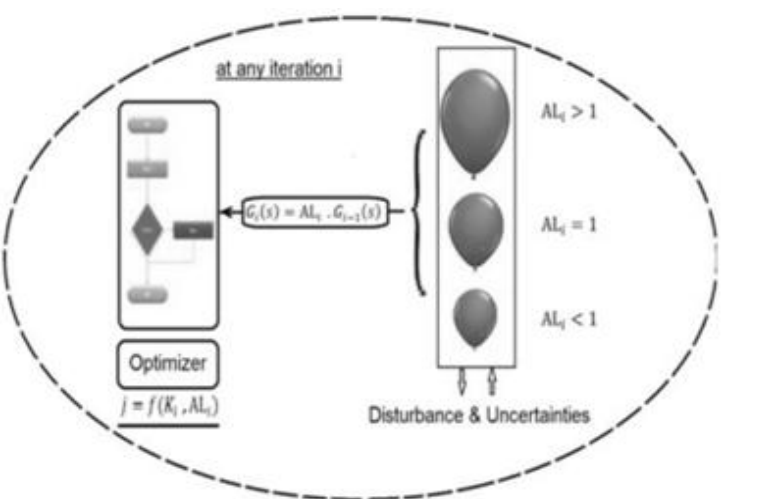


Fig. 3. Illustration of the BE mechanism for iterative gain adjustment under system disturbances [60]

2.4. Adaptive Modeling Using BE for Online Transfer Function Tuning

Fig. 4 depicts a streamlined MG configuration that facilitates the estimation of parameters for a second-order closed-loop system within the controlled region [60].

$$T.F = \frac{wn^2}{S^2 + 2\eta Wn + Wn^2} = \frac{\frac{Ki}{Mo}}{S^2 + \left(\frac{\left(Do + \frac{1}{Ro}\right)}{Mo}\right)S + \frac{Ki}{Mo}}$$
(15)

Here, Do, Ro, and M0 represent the nominal or reference values for the damping factor D, droop coefficient R, and inertia constant M, respectively.

$$\omega_n = \sqrt{\text{Ki/Mo}}, \ \eta = \frac{\frac{(Do + \frac{1}{Ro})}{Mo}}{2\omega_n}$$
 (16)

$$T_r = \frac{\pi - \sqrt{(1 - \eta^2)}}{\omega_n \sqrt{(1 - \eta^2)}}, \quad T_s = \frac{4}{\eta \omega_n}, M_P = e^{\frac{-\pi \eta}{\sqrt{(1 - \eta^2)}}}$$
 (17)

This expression defines the objective function formulated for the HHO-based identifier that incorporates the Balloon Effect mechanism.

$$J = min \sum (T_r + T_s + M_P)$$
 (18)

Accordingly, the objective function depends on the adaptive gain and the tuning coefficient, which are used to overcome system uncertainties and dynamic challenges.

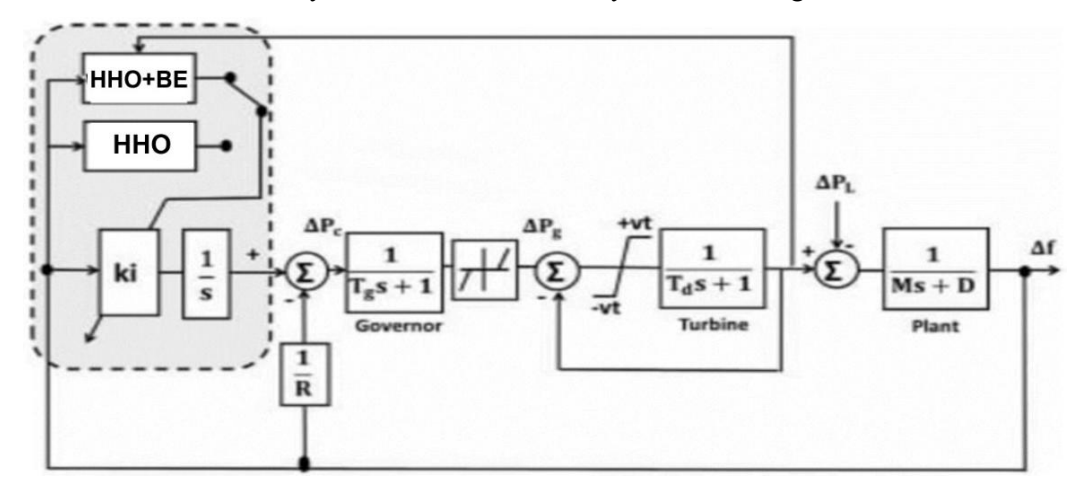


Fig. 4. Control architecture of the MG model with integrated HHO and BE mechanism

3. Results and Discussion

To assess the effectiveness of the proposed HHO+BE, a set of simulations was conducted using a representative isolated MG model composed of a 25 MW DG and a dynamically varying load. The MG's frequency response to different disturbances was studied to evaluate the capability of the adaptive controller in maintaining system stability. The system's dynamic behavior is governed by parameters such as inertia, damping, and governor time constants. These values were carefully selected to reflect realistic small-scale power systems and are summarized in Table 2. Furthermore, the optimization process for controller tuning was executed using four metaheuristic algorithms: HHO, GTO, SCA, and WOA. The specific parameter configurations for each optimizer are provided in Table 3, ensuring a fair and standardized comparison across all techniques. These parameters influence the convergence speed, exploration-exploitation balance, and the overall robustness of the optimization strategy.

3.1. Scenario 1: Load Disturbance Without Renewable Support

Under this scenario, the HHO+BE controller was evaluated under stringent operating constraints, specifically an islanded MG configuration relying solely on a 25 MW DG. To assess the controller's ability to manage frequency deviations, a ± 1.5 MW step change was applied to the nominal 15 MW load. The simulation outcomes underscore the controller's outstanding dynamic response. As depicted in Fig. 5, frequency fluctuations were confined to ± 0.18 Hz, with the system promptly stabilizing at 50 Hz in 8.4 seconds and exhibiting a negligible steady-state error of less than 0.01 Hz. Moreover, the controller achieved a rise time of 2.6 seconds and a peak response at 3.1 seconds, maintaining the lowest IAE across all methods at 0.74 Hz·s, according to Table 4.

Parameter	Symbol	Value	Unit	Description
System nominal frequency	fo	50	Hz	Base frequency of the MG
Rated power of the DG	P_DG	20	MW	Generator size
Governor time constant	\overline{T}_g	0.2	sec	Response time of the governor
Turbine time constant	T_t	0.3	sec	Response time of the diesel turbine
Inertia constant	\overline{M}	10	S	Equivalent system inertia
Damping coefficient	D	0.015	pu/Hz	Frequency sensitivity of load
Droop characteristic	R	2.4	Hz/pu	Frequency-power characteristic of the governor
Nominal load	P_L	15	MW	Average daily load
Load fluctuation range	=	± 1.5	MW	Step disturbance magnitude
Controller output gain	K_c	1	_	Initial gain for the control signal
Simulation time	_	100	sec	Total runtime for each test
Sampling time	_	0.01	sec	Time step for simulation resolution
BE initial gain	G_0	1	_	Nominal gain before adaptation
Balloon tuning sensitivity	k i	0.6	_	Scaling factor for system adaptation

Table 2. Designed system parameters for LFC simulation using HHO+BE

Table 3. Suggested parameters of HHO and comparative optimization algorithms

Parameter	ННО	GTO	SCA	WOA
Population size	30	30	30	30
Maximum iterations	100	100	100	100
Main control parameter	$E_0 \in [-1,1]$	$\beta = 3$, $\alpha = 0.03$	a = 2	a = 2
Position update strategy	Besiege & dive	Hierarchy-based	Sine-cosine update	Bubble-net & spiral
Exploration-exploitation switch	Based on E	By coefficients	Random-based	Switch probability
Randomness type	Lévy flights	Random leader- follower	Sinusoidal	Stochastic spiral
Notable feature	Escape energy adaptation	Troop dynamics	Simple sine behavior	Encircling behavior
Suitability for real-time use	High	Moderate	Low	Low-Moderate

Performance comparisons in Table 4 further validate HHO+BE's superiority. Competing algorithms such as GTO, SCA, and WOA displayed inferior characteristics, with frequency deviations reaching up to ±0.42 Hz, extended settling times (up to 18.9 seconds), and significantly higher IAE values. SCA, in particular, suffered from excessive overshoot and prolonged oscillations, resulting in the poorest control efficiency (IAE = 2.11 Hz·s). In terms of power regulation, Fig. 6 reveals that the HHO+BE strategy facilitated a smooth generator response, peaking at 21.8 MW before returning steadily to baseline. This was in contrast to the erratic power surges seen with controllers like SCA, which exceeded 23 MW (a sign of poor regulation and delayed stabilization). The performance summary in Table 5 indicates that HHO+BE consistently achieved the most favorable trade-off between response speed, control precision, and energy management. Altogether, these results affirm the effectiveness of embedding the BE into the HHO framework. This enhancement enables adaptive tuning, allowing the controller to swiftly counteract disturbances in isolated MGs or in contingency scenarios where renewable support is absent.

3.2. Scenario 2: Response Under Hybrid Generation with PV Integration

Building on the results from scenario 1, which featured DG-only operation, scenario 2 introduces a more realistic operating environment by incorporating PV generation. Here, approximately 30% of the 15 MW total demand (i.e., 4.5 MW) is supplied by PV, simulating typical daytime operation. This inclusion reduces system inertia and introduces solar-related variability, complicating the frequency regulation task. A step load change of ± 1.5 MW was again imposed. Additionally, PV generation was subjected to $\pm 5\%$ irradiance fluctuations, representing typical short-term variations. This compound disturbance scenario led to wider frequency excursions and demanded quicker controller adaptation.

Table 4.	Comparative	performance of	controllers under	load step (±1.	.5 MW)
----------	-------------	----------------	-------------------	----------------	--------

Technique	Max. Freq. Dev.	Settling time	IAE	Comment
HHO+BE	±0.18 Hz	8.4 s	0.74 Hz·s	Best overall stability & speed
GTO	$\pm 0.27~\mathrm{Hz}$	12.6 s	1.34 Hz·s	Moderate overshoot
SCA	±0.35 Hz	15.2 s	2.11 Hz·s	Fast convergence, weak damping
WOA	$\pm 0.42~Hz$	18.9 s	2.65 Hz·s	Poor settling, unstable recovery

Table 5. Summary of comparative performance ($\pm 1.5 \text{ MW}$)

Technique	Max. Freq. Dev.	Settling Time	Peak Power	IAE
SCA	±0.35 Hz	15.2 s	>23.0 MW	2.11 Hz·s
GTO	$\pm 0.27~\mathrm{Hz}$	12.6 s	22.5 MW	1.34 Hz·s
WOA	±0.42 Hz	18.9 s	22.8 MW	2.65 Hz·s
ННО	±0.24 Hz	10.1 s	21.9 MW	1.12 Hz·s
HHO + BE	$\pm 0.18~\mathrm{Hz}$	8.4 s	21.8 MW	0.74 Hz·s

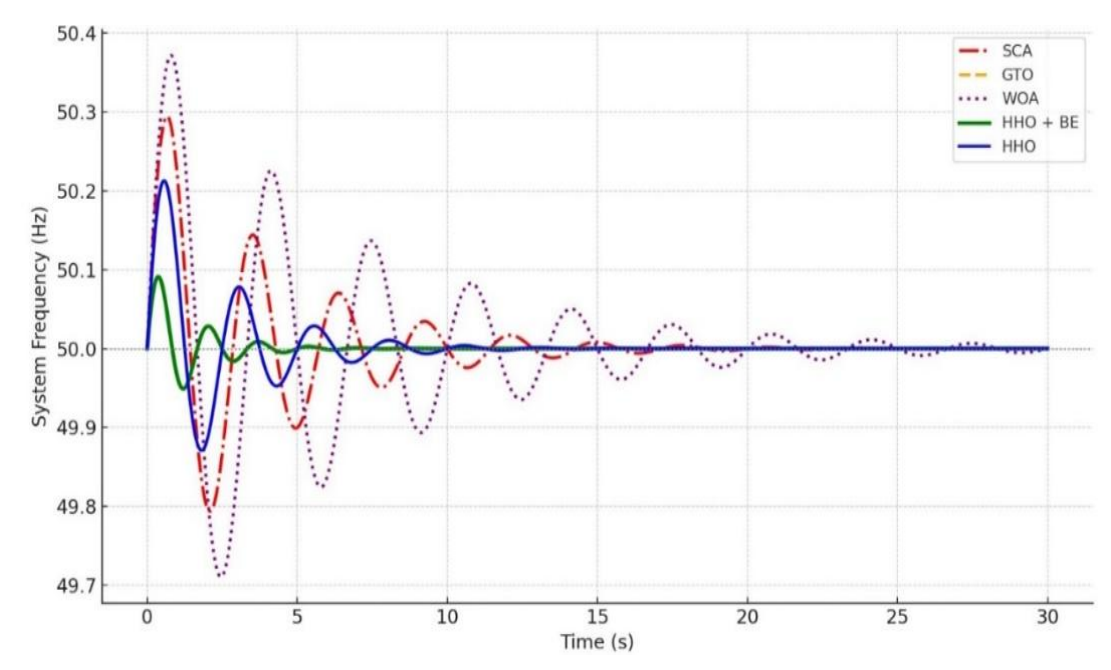


Fig. 5. Frequency deviation over time for various controllers

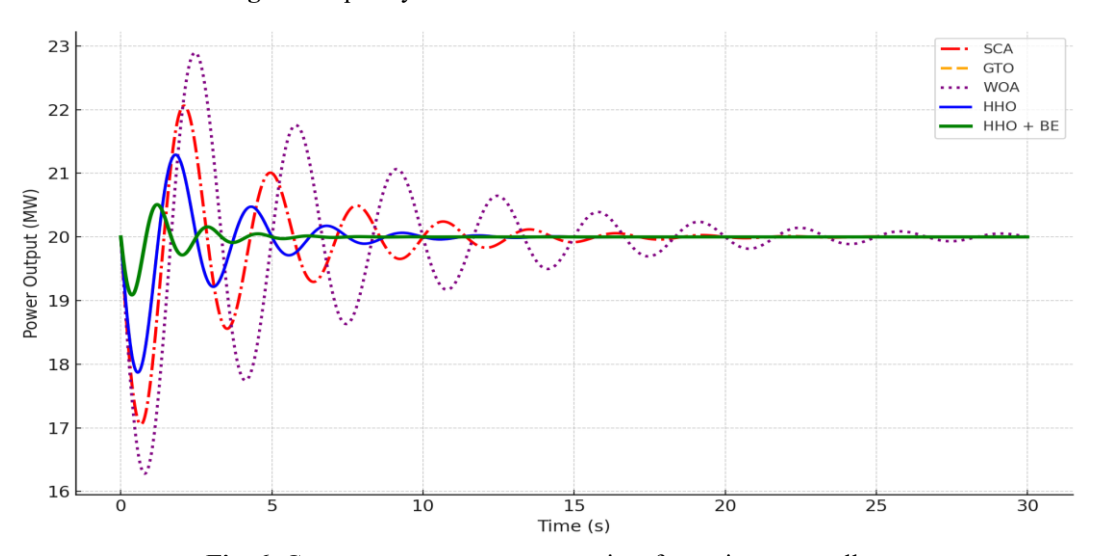


Fig. 6. Generator power output over time for various controllers

As shown in Fig. 7, the HHO+BE method succeeded in restricting frequency deviation to ± 0.22 Hz and restored the nominal frequency within 9.1 seconds. Although slightly slower than the 8.4 seconds seen in scenario 1, this still outpaced all benchmark algorithms. Table 6 summarizes the frequency response metrics for this hybrid setup. Power output data, illustrated in Fig. 8, shows that the DG's peak power reached 21.3 MW, thanks to PV sharing part of the load. In contrast, controllers like SCA and WOA triggered power spikes above 22.8 MW and exhibited prolonged oscillations, indicative of insufficient damping. These observations are further detailed in Table 6, comparing generator response and controller effectiveness across all tested strategies.

Overall, the results highlight the effectiveness of integrating the BE into the HHO framework. This mechanism dynamically tunes controller gains in real-time, enabling stable operation even under variable renewable input and sudden demand shifts. Such adaptability is vital for ensuring frequency stability and efficient energy management in hybrid MGs.

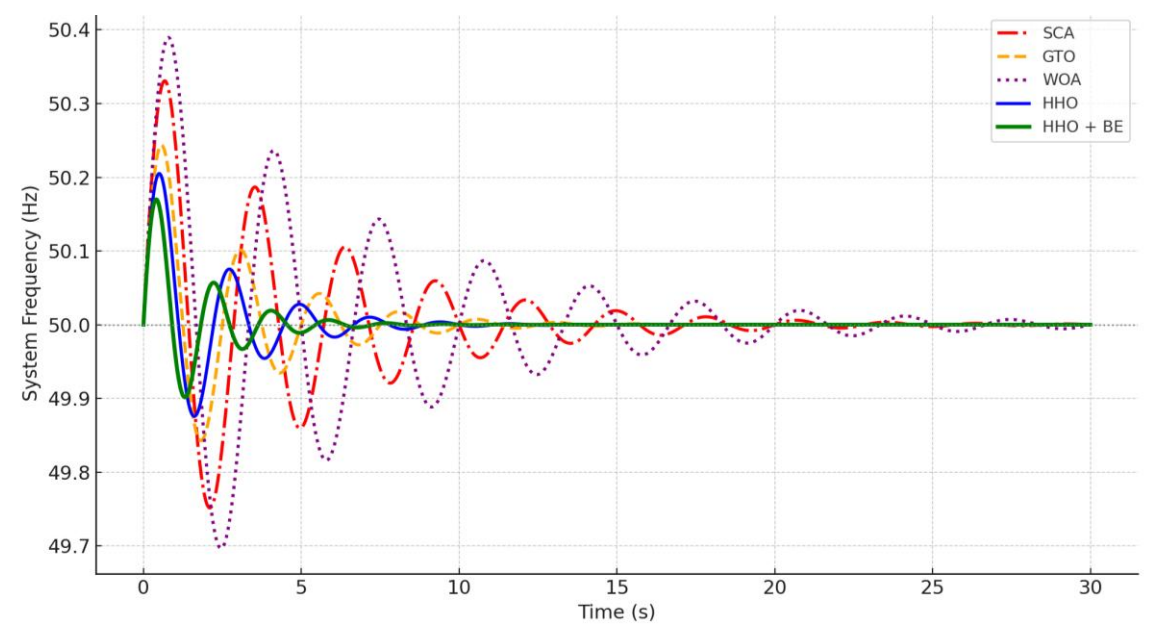


Fig. 7. Frequency response under PV integration scenario

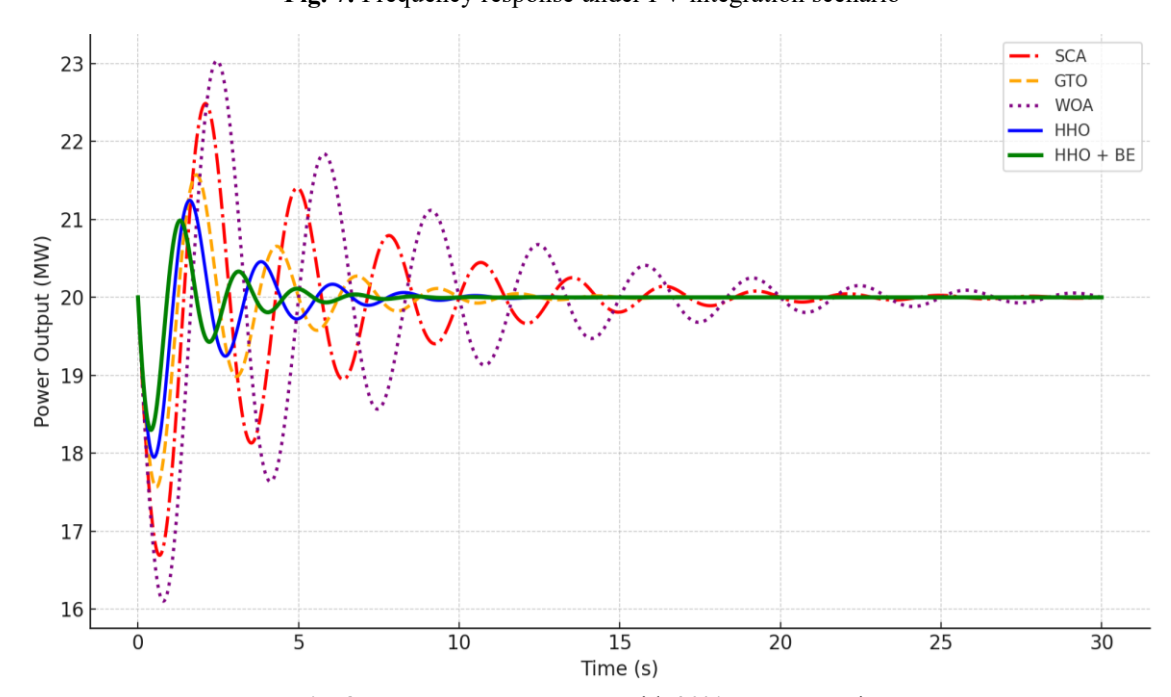


Fig. 8. Power output response with 30% PV penetration

Technique	Max. Frequency Deviations	Settling Time	Peak Power	IAE
SCA	±0.38 Hz	16.4 s	>22.8 MW	2.43 Hz·s
GTO	$\pm 0.30~\mathrm{Hz}$	13.5 s	22.1 MW	1.67 Hz·s
WOA	$\pm 0.44~\mathrm{Hz}$	19.2 s	22.4 MW	2.88 Hz·s
ННО	$\pm 0.26~\mathrm{Hz}$	10.7 s	21.6 MW	1.27 Hz·s
HHO + BE	±0.22 Hz	9.1 s	21.3 MW	0.91 Hz·s

Table 6. Comparative performance metrics – scenario 2 (30% PV penetration)

3.3. Scenario 3: Adaptive Control Under High Renewable Penetration and Parametric Uncertainty

Unlike the relatively structured conditions observed in the previous two scenarios, scenario 3 presents the most demanding and realistic test for MG frequency regulation. In this case, the system operates with 50% of its nominal 15 MW load (i.e., 7.5 MW) supplied by PV sources, while also being subjected to parametric uncertainties in core system characteristics: inertia ($\pm 20\%$), damping ($\pm 10\%$), and droop coefficients ($\pm 10\%$). This setup closely mirrors real-world challenges in weak grids dominated by renewables, where both source intermittency and model inaccuracies coexist.

Under these compounded conditions, system behavior diverged sharply from ideal responses. As shown in Fig. 9, frequency trajectories were highly irregular and aperiodic, lacking any consistent oscillatory pattern. This reflects the system's sensitivity to both structural uncertainty and renewable fluctuations. Traditional controllers such as SCA and WOA were unable to maintain stability, producing large deviations of up to ± 0.51 Hz and failing to achieve convergence within the 30-second simulation period, as detailed in Table 7. In contrast, the proposed HHO+BE controller retained commendable performance. It limited frequency variation to ± 0.28 Hz and restored nominal conditions within approximately 10.2 seconds. This success is attributed to the Balloon Effect mechanism, which enabled the controller to continuously adapt its tuning in response to shifting system parameters. As captured in Fig. 9, the frequency response of HHO+BE was significantly smoother and more contained compared to the volatile outputs of the benchmark algorithms.

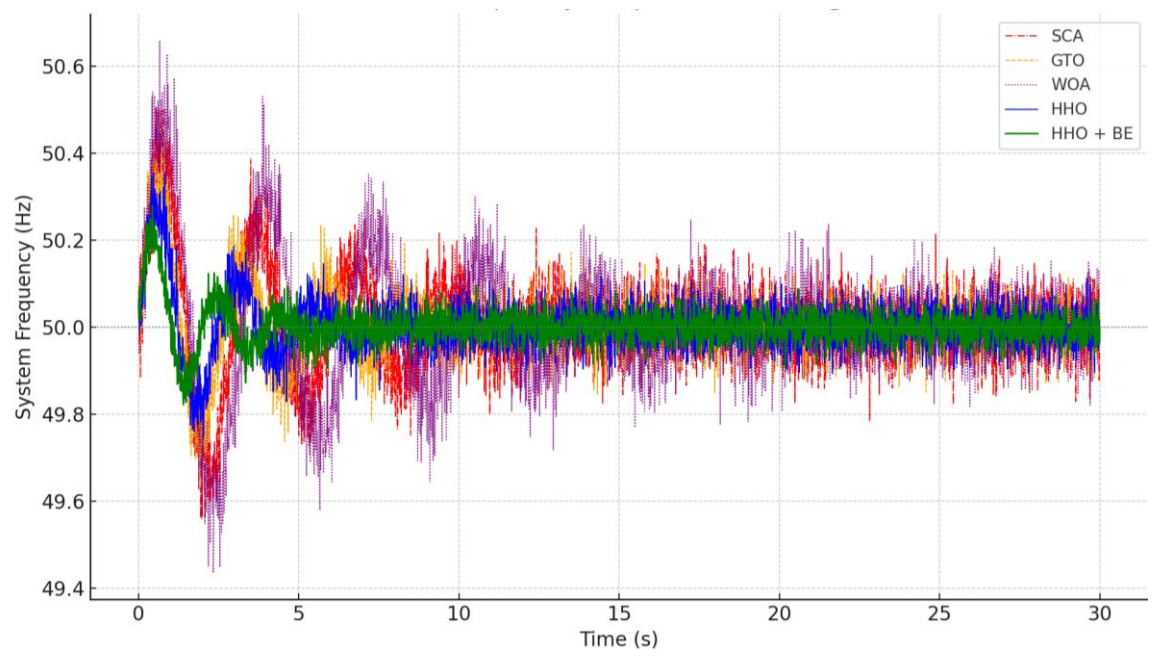


Fig. 9. Irregular frequency response under parameter uncertainty

The generator's power output pattern also supports these findings. Given the reduced inertia and 7.5 MW PV contribution, the diesel generator was forced to compensate dynamically. Fig. 10 illustrates how HHO+BE minimized overshoot and avoided excessive power surges, with a peak output of 17.6 MW, while WOA produced erratic control actions peaking at 18.15 MW, indicating inefficient power regulation. As summarized in Table 7, these results confirm that static control

strategies fall short under uncertain, renewable-dominant conditions. Adaptive methods (particularly those incorporating real-time gain adjustment like the HHO+BE) are essential for maintaining frequency and power stability in modern, low-inertia microgrid environments.

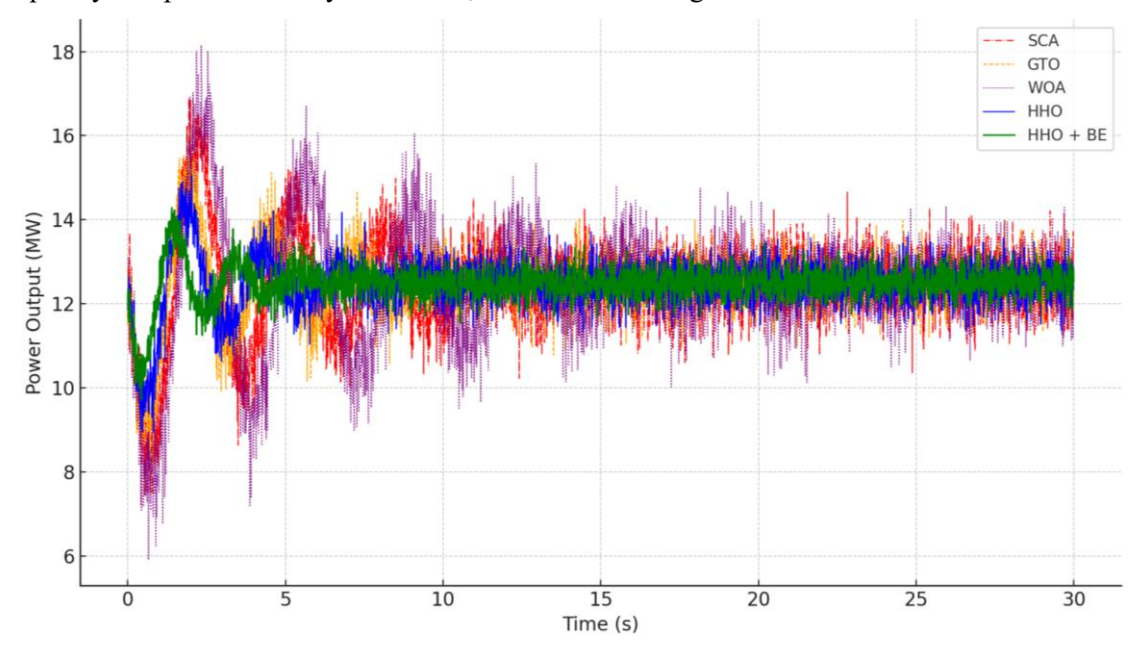


Fig. 10. Generator power output under uncertainty and high PV

Table 7. Performance comparison – scenario 3 (50% PV + Uncertainty)

Technique	Max Freq. Deviation	Settling Time	Peak Power	Stability Verdict
SCA	$\pm 0.46~\mathrm{Hz}$	>20 s	16.89 MW	Poor – failed to settle
GTO	±0.39 Hz	16.8 s	16.21 MW	Moderate
WOA	$\pm 0.51~\mathrm{Hz}$	>25 s	18.15 MW	Unstable – excessive power
HHO	$\pm 0.34~\mathrm{Hz}$	13.4 s	15.05 MW	Good – moderate performance
HHO + BE	$\pm 0.28~\mathrm{Hz}$	10.2 s	14.29 MW	Excellent – robust and adaptive

4. Conclusions

This research introduced a novel LFC approach tailored for hybrid MGs, leveraging the synergy between the HHO and the BE (HHO+BE). The controller's effectiveness was assessed under diverse operational conditions, including standalone DG operation, partial PV contribution, and scenarios with significant renewable integration coupled with system uncertainties. In all tested environments, the HHO+BE method consistently outperformed conventional optimization techniques like GTO, SCA, and WOA in terms of system response and robustness. The BE mechanism proved instrumental in enabling real-time adaptation to dynamic changes in load and system parameters, thereby enhancing control flexibility and reliability. The strategy achieved improved frequency stability, reduced deviation margins, and quicker convergence, particularly in cases involving high renewable shares and limited system inertia. Overall, the results confirm the potential of HHO+BE as a powerful tool for adaptive frequency control in future MGs. As the penetration of renewables continues to grow, such intelligent and responsive control methods will be crucial for preserving grid stability. Future research should explore hardware-based implementations and broader applications in interconnected MGs with energy storage systems and electric mobility integration.

Author Contribution: All authors contributed equally to the main contributor to this paper. All authors read and approved the final paper.

Sustainable Development Goals: Sustainable Development Goals mapped to this document, Affordable and Clean Energy Goal 7.

Data Availability: The data used to support the findings of this study are available at reasonable request from the corresponding author.

Conflicts of Interest: The authors declare that they have no conflicts of interest.

Acknowledgment: The authors extend their appreciation to Prince Sattam bin Abdulaziz University for funding this research work through the project number (PSAU/2025/01/33173).

Funding: The authors extend their appreciation to Prince Sattam bin Abdulaziz University for funding this research work through the project number (PSAU/2025/01/33173).

List of abbreviations

LFC : Load Frequency Control

PV : Photovoltaic

SCA : Sine Cosine AlgorithmHHO : Harris Hawks OptimizationDERs : Distributed Energy Resources

BE : Balloon Effect

MG : Microgrid

DG : Diesel Generator

GTO: Gorilla Troops Optimization
WOA: Whale Optimization Algorithm

HIL : Hardware-In-The-Loop

References

- [1] M. Awad *et al.*, "A review of water electrolysis for green hydrogen generation considering PV/wind/hydropower/geothermal/tidal and wave/biogas energy systems, economic analysis, and its application," *Alexandria Engineering Journal*, vol. 87, pp. 213-239, 2024, https://doi.org/10.1016/j.aej.2023.12.032.
- [2] Y. Maamar *et al.*, "A Comparative Analysis of Recent MPPT Algorithms (P&O\INC\FLC) for PV Systems," *Journal of Robotics and Control (JRC)*, vol. 6, no. 4, pp. 1581-1588, 2025, https://doi.org/10.18196/jrc.v6i4.25814.
- [3] M. S. Priyadarshini, S. A. E. M. Ardjoun, A. Hysa, M. M. Mahmoud, U. Sur, and N. Anwer, "Timedomain Simulation and Stability Analysis of a Photovoltaic Cell Using the Fourth-order Runge-Kutta Method and Lyapunov Stability Analysis," *Buletin Ilmiah Sarjana Teknik Elektro*, vol. 7, no. 2, pp. 214-230, 2025, https://doi.org/10.12928/biste.v7i2.13233.
- [4] M. Kiehbadroudinezhad, A. Merabet, C. Ghenai, A. G. Abo-Khalil, and T. Salameh, "The role of biofuels for sustainable MicrogridsF: A path towards carbon neutrality and the green economy," *Heliyon*, vol. 9, no. 2, p. e13407, 2023, https://doi.org/10.1016/j.heliyon.2023.e13407.
- [5] S. Heroual et al., "Enhancement of Transient Stability and Power Quality in Grid- Connected PV Systems Using SMES," *International Journal of Robotics and Control Systems*, vol. 5, no. 2, pp. 990-1005, 2025, https://doi.org/10.31763/ijrcs.v5i2.1760.
- [6] R. Kassem *et al.*, "A Techno-Economic-Environmental Feasibility Study of Residential Solar Photovoltaic / Biomass Power Generation for Rural Electrification: A Real Case Study," *Sustainability*, vol. 16, no. 5, p. 2036, 2024, https://doi.org/10.3390/su16052036.
- [7] S. Basu *et al.*, "Applications of Snow Ablation Optimizer for Sustainable Dynamic Dispatch of Power and Natural Gas Assimilating Multiple Clean Energy Sources," *Engineering Reports*, vol. 7, no. 6, p. e70211, 2025, https://doi.org/10.1002/eng2.70211.

- [8] T. Boutabba et al., "Design of a Small Wind Turbine Emulator for Testing Power Converters Using dSPACE 1104," International Journal of Robotics and Control Systems, vol. 5, no. 2, pp. 698-712, 2025, https://doi.org/10.31763/ijrcs.v5i2.1685.
- [9] A. Hysa, M. M. Mahmoud, and A. Ewais, "An Investigation of the Output Characteristics of Photovoltaic Cells Using Iterative Techniques and MATLAB ® 2024a Software," *Control Systems and Optimization Letters*, vol. 3, no. 1, pp. 46-52, 2025, https://doi.org/10.59247/csol.v3i1.174.
- [10] A. F. A. Ahmed, I. M. Elzein, M. M. Mahmoud, S. A. E. M. Ardjoun, A. M. Ewias, and U. Khaled, "Optimal Controller Design of Crowbar System for DFIG-based WT: Applications of Gravitational Search Algorithm," *Buletin Ilmiah Sarjana Teknik Elektro*, vol. 7, no. 2, pp. 122-137, 2025, https://doi.org/10.12928/biste.v7i2.13027.
- [11] P. Sinha *et al.*, "Efficient automated detection of power quality disturbances using nonsubsampled contourlet transform & PCA-SVM," *Energy Exploration & Exploitation*, vol. 43, no. 3, pp. 1149-1179, 2025, https://doi.org/10.1177/01445987241312755.
- [12] J. Sillman *et al.*, "Meta-analysis of climate impact reduction potential of hydrogen usage in 9 Power-to-X pathways," *Applied Energy*, vol. 359, p. 122772, 2024, https://doi.org/10.1016/j.apenergy.2024.122772.
- [13] A. Fatah *et al.*, "Design, and dynamic evaluation of a novel photovoltaic pumping system emulation with DS1104 hardware setup: Towards innovative in green energy systems," *PLoS One*, vol. 19, no. 10, p. e0308212, 2024, https://doi.org/10.1371/journal.pone.0308212.
- [14] H. M. I. Saleeb *et al.*, "Highly Efficient Isolated Multiport Bidirectional DC/DC Converter for PV Applications," *IEEE Access*, vol. 12, pp. 114480-114494, 2024, https://doi.org/10.1109/ACCESS.2024.3442711.
- [15] S. Ashfaq *et al.*, "Comparing the Role of Long Duration Energy Storage Technologies for Zero-Carbon Electricity Systems," *IEEE Access*, vol. 12, pp. 73169-73186, 2024, https://doi.org/10.1109/ACCESS.2024.3397918.
- [16] S. R. K. Joga *et al.*, "Applications of tunable-Q factor wavelet transform and AdaBoost classier for identification of high impedance faults: Towards the reliability of electrical distribution systems," *Energy Exploration* & *Exploitation*, vol. 42, no. 6, pp. 2017-2055, 2024, https://doi.org/10.1177/01445987241260949.
- [17] S. Shahzad, M. A. Abbasi, H. Ali, M. Iqbal, R. Munir, and H. Kilic, "Possibilities, Challenges, and Future Opportunities of Microgrids: A Review," *Sustainability*, vol. 15, no. 8, p. 6366, 2023, https://doi.org/10.3390/su15086366.
- [18] K. Feng and C. Liu, "Distributed Hierarchical Control for Fast Frequency Restoration in VSG-Controlled Islanded Microgrids," *IEEE Open Journal of the Industrial Electronics Society*, vol. 3, pp. 496-506, 2022, https://doi.org/10.1109/OJIES.2022.3202431.
- [19] P. Kumar and A. Singh Rana, "Review of optimization techniques for relay coordination in consideration with adaptive schemes of Microgrid," *Electric Power Systems Research*, vol. 230, p. 110240, 2024, https://doi.org/10.1016/j.epsr.2024.110240.
- [20] M. N. A. Hamid, "Adaptive Frequency Control of an Isolated Microgrids Implementing Different Recent Optimization Techniques," *International Journal of Robotics and Control Systems*, vol. 4, no. 3, pp. 1000-1012, 2024, https://doi.org/10.31763/ijrcs.v4i3.1432.
- [21] M. Awad, M. M. Mahmoud, Z. M. S. Elbarbary, L. Mohamed Ali, S. N. Fahmy, and A. I. Omar, "Design and analysis of photovoltaic/wind operations at MPPT for hydrogen production using a PEM electrolyzer: Towards innovations in green technology," *PLoS One*, vol. 18, no. 7, p. e0287772, 2023, https://doi.org/10.1371/journal.pone.0287772.
- [22] G. Di Luca, G. Di Blasio, A. Gimelli, and D. A. Misul, "Review on Battery State Estimation and Management Solutions for Next-Generation Connected Vehicles," *Energies*, vol. 17, no. 1, p. 202, 2024, https://doi.org/10.3390/en17010202.
- [23] K. Peddakapu, M. R. Mohamed, P. Srinivasarao, Y. Arya, P. K. Leung, and D. J. K. Kishore, "A state-of-the-art review on modern and future developments of AGC/LFC of conventional and renewable

- energy-based power systems," *Renewable Energy Focus*, vol. 43. pp. 146-171, 2022, https://doi.org/10.1016/j.ref.2022.09.006.
- [24] S. Zeinal-Kheiri, A. M. Shotorbani and B. Mohammadi-Ivatloo, "Real-time Energy Management of Grid-connected Microgrid with Flexible and Delay-tolerant Loads," *Journal of Modern Power Systems and Clean Energy*, vol. 8, no. 6, pp. 1196-1207, 2020, https://doi.org/10.35833/MPCE.2018.000615.
- [25] A. A. Heidari, S. Mirjalili, H. Faris, I. Aljarah, M. Mafarja, and H. Chen, "Harris hawks optimization: Algorithm and applications," *Future Generation Computer Systems*, vol. 97, pp. 849-872, 2019, https://doi.org/10.1016/j.future.2019.02.028.
- [26] M. M. Mahmoud *et al.*, "Voltage Quality Enhancement of Low-Voltage Smart Distribution System Using Robust and Optimized DVR Controllers: Application of the Harris Hawks Algorithm," *International Transactions on Electrical Energy Systems*, vol. 2022, no. 1, pp. 1-18, 2022, https://doi.org/10.1155/2022/4242996.
- [27] P. Attiwal and S. Indora, "A Comprehensive Review of Modern Methods for Load Prediction in the Smart Grid," *Recent Patents on Engineering*, vol. 18, no. 4, 2024, http://dx.doi.org/10.2174/1872212118666230423143331.
- [28] S. Heroual, B. Belabbas, Y. Diab, M. M. Mahmoud, T. Allaoui, and N. Benabdallah, "Optimizing Power Flow in Photovoltaic-Hybrid Energy Storage Systems: A PSO and DPSO Approach for PI Controller Tuning," *International Transactions on Electrical Energy Systems*, vol. 2025, no. 1, pp. 1-23, 2025, https://doi.org/10.1155/etep/9958218.
- [29] B. Krishna Ponukumati *et al.*, "Evolving fault diagnosis scheme for unbalanced distribution network using fast normalized cross-correlation technique," *PLoS One*, vol. 19, no. 10, p. e0305407, 2024, https://doi.org/10.1371/journal.pone.0305407.
- [30] V. Kumar *et al.*, "A Novel Hybrid Harris Hawk Optimization-Sine Cosine Transmission Network," *Energies*, vol. 17, no. 19, p. 4985, 2024, https://doi.org/10.3390/en17194985.
- [31] H. Shayeghi and A. Younesi, "Mini/micro-grid adaptive voltage and frequency stability enhancement using Q-learning mechanism through the offset of PID controller," *Journal of Operation and Automation in Power Engineering*, vol. 7, no. 1, pp. 107-118, 2019, https://joape.uma.ac.ir/article_764_81351c0790c86bdb54864629a0e2b4d4.pdf.
- [32] A. H. Elmetwaly *et al.*, "Modeling, Simulation, and Experimental Validation of a Novel MPPT for Hybrid Renewable Sources Integrated with UPQC: An Application of Jellyfish Search Optimizer," *Sustainability*, vol. 15, no. 6, p. 5209, 2023, https://doi.org/10.3390/su15065209.
- [33] N. F. Ibrahim *et al.*, "Multiport Converter Utility Interface with a High-Frequency Link for Interfacing Clean Energy Sources (PV\Wind\Fuel Cell) and Battery to the Power System: Application of the HHA Algorithm," *Sustainability*, vol. 15, no. 18, p. 13716, 2023, https://doi.org/10.3390/su151813716.
- [34] M. M. Elymany, M. A. Enany, and N. A. Elsonbaty, "Hybrid optimized-ANFIS based MPPT for hybrid microgrid using zebra optimization algorithm and artificial gorilla troops optimizer," *Energy Conversion and Management*, vol. 299, p. 117809, 2024, https://doi.org/10.1016/j.enconman.2023.117809.
- [35] N. F. Nanyan, M. A. Ahmad, and B. Hekimoğlu, "Optimal PID controller for the DC-DC buck converter using the improved sine cosine algorithm," *Results in Control and Optimization*, vol. 14, p. 100352, 2024, https://doi.org/10.1016/j.rico.2023.100352.
- [36] M. M. Mahmoud, M. K. Ratib, M. M. Aly, and A. M. M. Abdel–Rahim, "Application of Whale Optimization Technique for Evaluating the Performance of Wind-Driven PMSG Under Harsh Operating Events," *Process Integration and Optimization for Sustainability*, vol. 6, pp. 447-470, 2022, https://doi.org/10.1007/s41660-022-00224-8.
- [37] G. Sahoo, R. K. Sahu, S. Panda, N. R. Samal, and Y. Arya, "Modified Harris Hawks Optimization-Based Fractional-Order Fuzzy PID Controller for Frequency Regulation of Multi-Micro-Grid," *Arabian Journal for Science and Engineering*, vol. 48, no. 11, pp. 14381-14405, 2023, https://doi.org/10.1007/s13369-023-07613-2.

- [38] Y. L. Karnavas and E. Nivolianiti, "Harris hawks optimization algorithm for load frequency control of isolated multi-source power generating systems," *International Journal of Emerging Electric Power Systems*, vol. 25, no. 4, pp. 555-571, 2024, https://doi.org/10.1515/ijeeps-2023-0035.
- [39] R. Pachaiyappan, E. Arasan, and K. Chandrasekaran, "Improved Gorilla Troops Optimizer-Based Fuzzy PD-(1+PI) Controller for Frequency Regulation of Smart Grid under Symmetry and Cyber Attacks," *Symmetry*, vol. 15, no. 11, p. 2013, 2023, https://doi.org/10.3390/sym15112013.
- [40] N. F. Ibrahim, A. Alkuhayli, A. Beroual, U. Khaled, and M. M. Mahmoud, "Enhancing the Functionality of a Grid-Connected Photovoltaic System in a Distant Egyptian Region Using an Optimized Dynamic Voltage Restorer: Application of Artificial Rabbits Optimization," *Sensors*, vol. 23, no. 16, p. 7146, 2023, https://doi.org/10.3390/s23167146.
- [41] F. Menzri *et al.*, "Applications of Novel Combined Controllers for Optimizing Grid-Connected Hybrid Renewable Energy Systems," *Sustainability*, vol. 16, no. 16, p. 6825, 2024, https://doi.org/10.3390/su16166825.
- [42] M. M. Mahmoud *et al.*, "Application of Whale Optimization Algorithm Based FOPI Controllers for STATCOM and UPQC to Mitigate Harmonics and Voltage Instability in Modern Distribution Power Grids," *Axioms*, vol. 12, no. 5, p. 420, 2023, https://doi.org/10.3390/axioms12050420.
- [43] M.-H. Khooban *et al.*, "Robust Frequency Regulation in Mobile Microgrids: HIL Implementation," *IEEE Systems Journal*, vol. 13, no. 4, pp. 4281-4291, 2019, https://doi.org/10.1109/JSYST.2019.2911210.
- [44] M. Rezaeimozafar, M. Eskandari and A. V. Savkin, "A Self-Optimizing Scheduling Model for Large-Scale EV Fleets in Microgrids," *IEEE Transactions on Industrial Informatics*, vol. 17, no. 12, pp. 8177-8188, 2021, https://doi.org/10.1109/TII.2021.3064368.
- [45] G. Li, Y. Jin, M. W. Akram, X. Chen, and J. Ji, "Application of bio-inspired algorithms in maximum power point tracking for PV systems under partial shading conditions A review," *Renewable and Sustainable Energy Reviews*, vol. 81. pp. 840-873, 2018, https://doi.org/10.1016/j.rser.2017.08.034.
- [46] N. F. Ibrahim *et al.*, "Operation of Grid-Connected PV System With ANN-Based MPPT and an Optimized LCL Filter Using GRG Algorithm for Enhanced Power Quality," *IEEE Access*, vol. 11, pp. 106859-106876, 2023, https://doi.org/10.1109/ACCESS.2023.3317980.
- [47] I. El Maysse *et al.*, "Nonlinear Observer-Based Controller Design for VSC-Based HVDC Transmission Systems Under Uncertainties," *IEEE Access*, vol. 11, pp. 124014-124030, 2023, https://doi.org/10.1109/ACCESS.2023.3330440.
- [48] K. Shinde and P. B. Mane, "Review on high penetration of rooftop solar energy with secondary distribution networks using smart inverter," *Energy Reports*, vol. 8. pp. 5852-5860, 2022, https://doi.org/10.1016/j.egyr.2022.03.086.
- [49] H. Boudjemai *et al.*, "Design, Simulation, and Experimental Validation of a New Fuzzy Logic-Based Maximal Power Point Tracking Strategy for Low Power Wind Turbines," *International Journal of Fuzzy Systems*, vol. 26, pp. 2567-2584, 2024, https://doi.org/10.1007/s40815-024-01747-7.
- [50] A. T. Hassan *et al.*, "Adaptive Load Frequency Control in Microgrids Considering PV Sources and EVs Impacts: Applications of Hybrid Sine Cosine Optimizer and Balloon Effect Identifier Algorithms," *International Journal of Robotics and Control Systems*, vol. 4, no. 2, pp. 941-957, 2024, https://doi.org/10.31763/ijrcs.v4i2.1448.
- [51] O. M. Kamel, A. A. Z. Diab, M. M. Mahmoud, A. S. Al-Sumaiti, and H. M. Sultan, "Performance Enhancement of an Islanded Microgrid with the Support of Electrical Vehicle and STATCOM Systems," *Energies*, vol. 16, no. 4, p. 1577, 2023, https://doi.org/10.3390/en16041577.
- [52] N. F. Ibrahim *et al.*, "A new adaptive MPPT technique using an improved INC algorithm supported by fuzzy self-tuning controller for a grid-linked photovoltaic system," *PLoS One*, vol. 18, no. 11, p. e0293613, 2023, https://doi.org/10.1371/journal.pone.0293613.
- [53] O. M. Lamine *et al.*, "A Combination of INC and Fuzzy Logic-Based Variable Step Size for Enhancing MPPT of PV Systems," *International Journal of Robotics and Control Systems*, vol. 4, no. 2, pp. 877-892, 2024, https://doi.org/10.31763/ijrcs.v4i2.1428.

- [54] A. G. Hussien *et al.*, "Recent Advances in Harris Hawks Optimization: A Comparative Study and Applications," *Electronics*, vol. 11, no. 12, p. 1919, 2022, https://doi.org/10.3390/electronics11121919.
- [55] J. You *et al.*, "Modified Artificial Gorilla Troop Optimization Algorithm for Solving Constrained Engineering Optimization Problems," *Mathematics*, vol. 11, no. 5, p. 1256, 2023, https://doi.org/10.3390/math11051256.
- [56] R. M. Rizk-Allah and A. E. Hassanien, "A comprehensive survey on the sine—cosine optimization algorithm," *Artificial Intelligence Review*, vol. 56, no. 6, pp. 4801-4858, 2023, https://doi.org/10.1007/s10462-022-10277-3.
- [57] S. Mahmood, N. Z. Bawany, and M. R. Tanweer, "A comprehensive survey of whale optimization algorithm: modifications and classification," *Indonesian Journal of Electrical Engineering and Computer Science (IJEECS)*, vol. 29, no. 2, pp. 899-910, 2023, http://doi.org/10.11591/ijeecs.v29.i2.pp899-910.
- [58] M. M. Hussein, T. H. Mohamed, M. M. Mahmoud, M. Aljohania, M. I. Mosaad, and A. M. Hassan, "Regulation of multi-area power system load frequency in presence of V2G scheme," *PLoS One*, vol. 18, no. 9, p. e0291463, 2023, https://doi.org/10.1371/journal.pone.0291463.
- [59] A. M. Ewais, A. M. Elnoby, T. H. Mohamed, M. M. Mahmoud, Y. Qudaih, and A. M. Hassan, "Adaptive frequency control in smart microgrid using controlled loads supported by real-time implementation," *PLoS One*, vol. 18, no. 4, p. e0283561, 2023, https://doi.org/10.1371/journal.pone.0283561.
- [60] A. M. Ewias *et al.*, "Advanced load frequency control of microgrid using a bat algorithm supported by a balloon effect identifier in the presence of photovoltaic power source," *PLoS One*, vol. 18, no. 10, p. e0293246, 2023, https://doi.org/10.1371/journal.pone.0293246.
- [61] H. Gezici and H. Livatyali, "Chaotic Harris hawks optimization algorithm," *Journal of Computational Design and Engineering*, vol. 9, no. 1, pp. 216-245, 2022, https://doi.org/10.1093/jcde/qwab082.
- [62] C. Li, Q. Si, J. Zhao, and P. Qin, "A robot path planning method using improved Harris Hawks optimization algorithm," *Measurement and Control*, vol. 57, no. 4, pp. 469-482, 2024, https://doi.org/10.1177/00202940231204424.
- [63] H. Kang, R. Liu, Y. Yao, and F. Yu, "Improved Harris hawks optimization for non-convex function optimization and design optimization problems," *Mathematics and Computers in Simulation*, vol. 204, pp. 619-639, 2023, https://doi.org/10.1016/j.matcom.2022.09.010.
- [64] M. M. Hussein, M. N. A. Hamid, T. H. Mohamed, I. M. Al-Helal, A. Alsadon, and A. M. Hassan, "Advanced Frequency Control Technique Using GTO with Balloon Effect for Microgrids with Photovoltaic Source to Lower Harmful Emissions and Protect Environment," *Sustainability*, vol. 16, no. 2, p. 831, 2024, https://doi.org/10.3390/su16020831.
- [65] T. H. Mohamed, M. A. M. Alamin, and A. M. Hassan, "A novel adaptive load frequency control in single and interconnected power systems," *Ain Shams Engineering Journal*, vol. 12, no. 2, pp. 1763-1773, 2021, https://doi.org/10.1016/j.asej.2020.08.024.